LBL-12178
Preprint

Lawrence Berkeley Laboratory
UNIVERSITY OF CALIFORNIA

Materials & Molecular
Research Division

Submitted to the Journal of Catalysis

SYNTHESIS OF OXYGENATED PRODUCTS FROM CARBON MONOXIDE AND HYDROGEN OVER SILICA- AND ALUMINA-SUPPORTED RUTHENIUM CATALYSTS

C. Stephen Kellner and Alexis T. Bell

March 1981

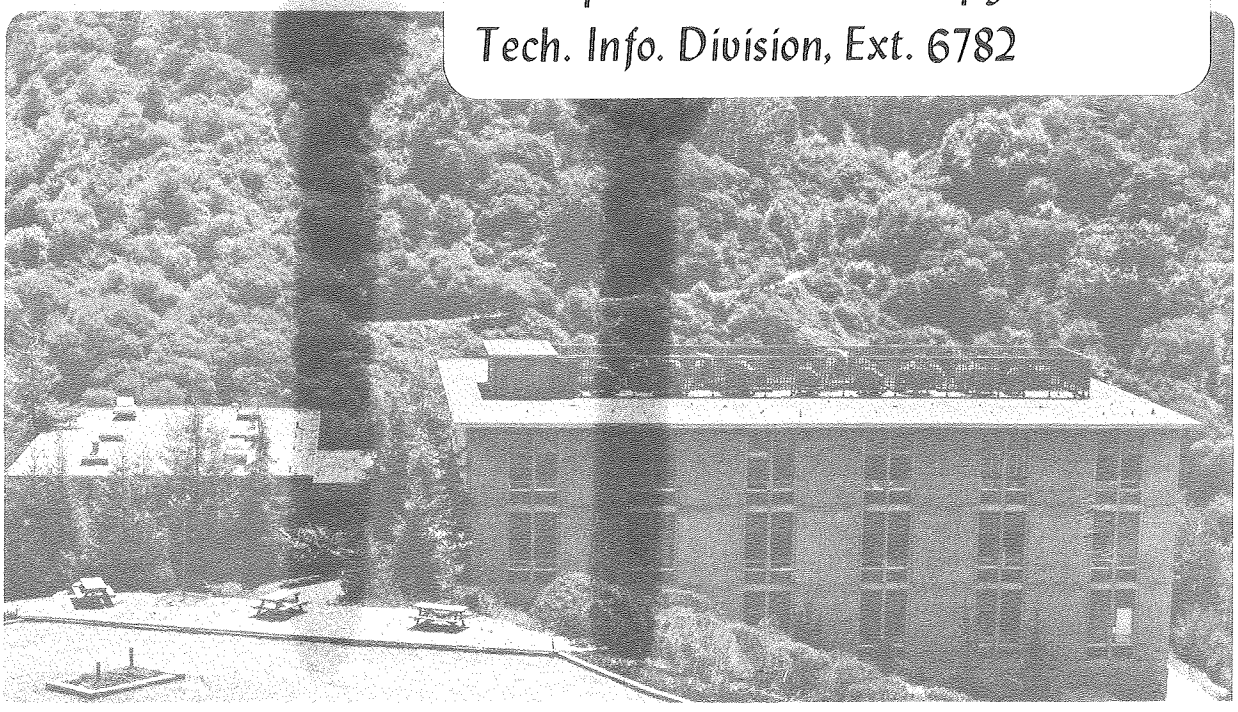

Prepared for the U.S. Department of Energy under Contract W-7405-ENG-48

DISCLAIMER

LBL-12178

Synthesis of Oxygenated Products from Carbon Monoxide and Hydrogen Over Silica- and Alumina-Supported Ruthenium Catalysts

by

C. Stephen Kellner and Alexis T. Bell

Materials and Molecular Research Division
Lawrence Berkeley Laboratory

and

Department of Chemical Engineering
University of California, Berkeley, California 94720

Submitted to

Journal of Catalysis

ABSTRACT

The synthesis of oxygenated products over supported ruthenium catalysts was investigated using both H_2/CO and D_2/CO feed mixtures. Acetaldehyde was the principal oxygenated product formed over silica-supported ruthenium. By contrast, methanol was the principal oxygenated species formed over an alumina-supported catalyst. A significant inverse H_2/D_2 isotope effect was observed on the rate of formation of both acetaldehyde and methanol. The kinetics of acetaldehyde synthesis were determined and compared with those for methane synthesis. The form of the rate expressions obtained for each product and the origins of the observed isotope effects are explained in terms of a mechanism for the synthesis of both products. A reaction mechanism for methanol synthesis is also proposed.

INTRODUCTION

It is well recognized that oxygenated products such as alcohols, aldehydes, acids, etc. are produced in parallel with hydrocarbons during Fischer-Tropsch synthesis over iron and cobalt catalysts (1). By contrast, though, very little is known about the synthesis of oxygenated compounds over ruthenium. The purpose of the present investigation was to establish the activity of Ru/SiO_2 and Ru/Al_2O_3 catalysts for the synthesis of such compounds and to shed some light on the mechanisms by which these products are formed. For this purpose rate data were acquired, over a broad range of reaction conditions, using both H_2/CO and D_2/CO feed mixtures.

EXPERIMENTAL

Preparation of the 1.2% Ru/SiO_2 and 1.0% Ru/Al_2O_3 catalysts used in this study have been described in detail elsewhere (2,3). The initial dispersion of the alumina-supported catalyst determined by H_2 chemisorption, was found to be near unity. Measurements of dispersion following use of this catalyst showed that the dispersion gradually decreased to about 0.6 and remained fairly constant thereafter. The dispersion of the silica-supported catalyst could not be determined by H_2 chemisorption since the uptake of H_2, even at elevated temperatures, was exceedingly slow, and hence the point at which equilibrium was attained could not be established reliably. As a result, the dispersion of this catalyst was measured by CO chemisorption and determined to be 0.25, based on the assumption that the ratio of CO to surface Ru atoms is unity. The validity of this assumption is supported by previous studies with low dispersion Ru/Al_2O_3 catalysts (5) and by the observation that infrared spectra of CO adsorbed on the Ru/SiO_2 used in this study (6) show only a single band, attributable to linearly adsorbed CO.

The experimental apparatus and procedure have been described previously (2). All of the experiments were carried out in a stainless

steel microreactor heated in a fluidized bed. A premixed feed composed of $H_2(D_2)$ and CO at a ratio of $H_2(D_2)/CO = 3.0$ was supplied to the reactor and the product gas was analyzed by a gas chromatograph equipped with flame ionization detectors. The detector sensitivities for deuterated and hydrogenated products were established to be identical by injecting pure samples of CH_4 and CD_4.

Each experiment with a fresh catalyst charge (100 mg) was initiated by a 10 to 12 hr reduction in flowing H_2 at 673K and 10 atm. The temperature was then lowered to 498K and the feed mixture was introduced at a flow rate of 200 cm^3/min (NTP). Ten minutes after the reaction began, a gas sample was taken for analysis and the gas feed was switched over to pure H_2 for 1 hr. By alternating short reaction periods and longer reduction periods, a stable catalyst activity could be achieved after several cycles. Once this status was attained, the catalyst was cooled to 453K and data were taken between 453 and 498K. The catalyst was then heated to 548K, and data were taken between 548 and 498K. By following this procedure, a check could be obtained for catalyst deactivation. In all cases the reaction rate measured at 498K could be reproduced to within a few percent. It should be noted further, that in all instances the conversion of CO was low, ranging from 0.02% at 453K to 1.5% at 548K.

RESULTS

Ru/SiO_2

The primary oxygen-containing organic product proudced over the Ru/SiO_2 catalyst was acetaldehyde. Measurements of the rate of formation of this product as well as the rate of methane formation were obtained at pressures of 1 and 10 atm, over the temperature range of 448 to 548K, using H_2/CO ratios of 1 and 3. The kinetics for producing both products could be

represented by power law expressions, and the constants appearing in these relations were determined by means of a nonlinear least-squares regression analysis. The resulting expression for acetaldehyde is given by

$$N_{CH_3CHO} = 7.1 \times 10^2 P_{H_2}^{0.6} \exp(-15{,}000/RT) \qquad (1)$$

and that for methane by

$$N_{CH_4} = 8.0 \times 10^9 P_{H_2}^{1.3} P_{CO}^{-1.0} \exp(-29{,}600/RT). \qquad (2)$$

In both equations, the rates of acetaldehyde and methane synthesis, N_{CH_3CHO} and N_{CH_4}, are expressed in molecules of product produced per second per Ru surface site, and the partial pressures of H_2 and CO, P_{H_2} and P_{CO}, are expressed in atmospheres. Deviations of less than $\pm$ 7% were observed between the rates predicted by eqns. 1 and 2 and the rates of each product observed experimentally. It is of further interest to note that eqn. 2 is in very good agreement with the rate expression recently reported for methane synthesis over the Ru/Al_2O_3 catalyst used in the present studies (4).

Substitution of D_2 for H_2 in the synthesis gas mixture affects the rates of acetaldehyde and methane formation. Figure 1a shows Arrhenius plots for the formation of acetaldehyde from H_2/CO and D_2/CO mixtures at 1 and 10 atm. At both pressures the rate of acetaldehyde formation is seen to be approximately twice as rapid when D_2 rather than H_2 is present in the feed. Figure 1b shows that the rate of methane formation is influenced to a much lesser degree when D_2 is substituted for H_2. At 10 atm, the rate of CD_4 formation is approximately 1.1 times that observed for CH_4; however, no isotope effect can be observed at 1 atm.

$\underline{Ru/Al_2O_3}$

In contrast to the Ru/SiO_2 catalyst, the Ru/Al_2O_3 catalyst was active for the formation of methanol but produced very little acetaldehyde. For a given temperature, pressure, and H_2/CO ratio, the rate of methanol formation was found to be a strong function of the feed flow rate. As shown in Fig. 2, the observed rate of methanol formation increases substantially with increasing flow rate and approaches a plateau at high flow rates. Since the rate of forming methane and C_{2+} hydrocarbons is unaffected by flow rate, the trend observed in Fig. 2 suggests that at low flow rates, a part of the methanol formed decomposes back to CO and H_2 or reacts with the alumina support to form formates (7). The duration of each experiment also has a strong influence on the production of methanol. Figure 3 shows that the rate of methanol synthesis increases from practically zero to an asymptotic level, over a 20 min period. During the same interval, the rate of methane formation declines by about a third. While not shown, a similar decline was also observed in the formation of C_{2+} products. The similarities in the dynamics of the deactivation of the catalyst for hydrocarbon synthesis and its apparent activation for methanol synthesis suggest that the latter trend is due to a progressive poisoning or deactivation of the catalyst sites responsible for methanol decomposition.

The influence of total pressure and H_2/CO ratio on the synthesis of methane and methanol is presented in Table I. As can be seen, both rates increase with increasing pressure and H_2/CO ratio. The formation of methanol relative to methane is favored at high pressures, but the H_2/CO ratio has only a negligible influence on the product selectivity ratio. The effects of temperature on the rates of methanol and methane synthesis are shown in Fig. 4. The apparent activation energies for

methanol and methane synthesis determined from these data are 21.6 and 28 kcal/mole, respectively. Arrhenius plots for the synthesis of methanol and methane from D_2 and CO are also shown in Fig. 4. Utilization of D_2 in the feed gas increases the absolute rate of methanol synthesis by a factor of 1.6 over that observed for a feed containing H_2 and CO and increases the rate of methane formation by a factor of 1.4.

DISCUSSION

The mechanism of acetaldehyde formation can be envisioned as an extension of the mechanism recently proposed (4,8) to explain the synthesis of hydrocarbons over Ru catalysts. Since detailed discussions of the steps entering the latter scheme have already been presented, only a brief summary will be given here. As may be seen in Fig. 5, the synthesis of hydrocarbons is initiated by dissociative chemisorption of CO and H_2. Stepwise hydrogenation of the atomic carbon, released by CO dissociation, results in the formation of methyl groups. These species then act as precursors to the formation of both methane and C_{2+} olefins and paraffins. The first of these products is formed by hydrogen addition to the methyl group, while the growth of hydrocarbon chains is initiated by the addition of a methylene group. Olefins and paraffins are formed by either β-hydrogen elimination from or, α-hydrogen addition to, the adsorbed alkyl intermediates. The formation of acetaldehyde is proposed to occur via a two step process. In the first, CO is inserted into the metal-carbon bond of a methyl group. The addition of hydrogen to the resulting acetyl group then produces acetaldehyde in the second step. It should be noted that higher molecular weight aldehydes could be formed via similar processes starting with alkyl groups containing two or more carbon atoms.

The proposed mechanism of acetaldehyde formation is supported by a number of precedents originating in the field of coordination chemistry. The insertion of CO into the metal-carbon bond of transition metal complexes, containing methyl ligands, is well documented (9,10) and is believed to occur via migration of the methyl group to form an acetyl group (9). CO insertion has also been demonstrated to occur during the hydroformylation of ethylene, catalyzed by transition metal complexes (11). The formation of acetyl derivatives has been reported via the reaction of $CH_3RuCp(CO)_2$ in the presence of tertiary phosphines. It has been noted (9,12), though, that these acryl complexes are not as stable as those produced with metals appearing further to the left in the transition series. Acetyl derivatives can also be formed from acetaldehyde. Thus, for example (13), the reaction of $Os(CO)_2(PPh)_3$ with excess acetaldehyde produces structure I.

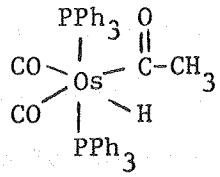

(I)

In view of this result and the concept of microreversability, it seems reasonable to suggest that the formation of acetaldehyde can occur by reductive elimination of an acetyl group (step 13 in Fig. 5).

If it is assumed that reactions 8 and 12 are the rate limiting steps for the formation of methane and acetaldehyde, respectively, then the rate of formation of each product can be described by eqns. 3 and 4.

$$N_{CH_4} = k_8 \theta_{CH_3} \theta_H \quad (3)$$

$$N_{CH_3CHO} = k_{12} \theta_{CH_3} \theta_{CO} \quad (4)$$

where k_8 and k_{12} are the rate coefficients for reactions 8 and 12, respectively, and θ_{CH_3}, θ_H, and θ_{CO} are the fractional coverages of the catalyst surface by adsorbed CH_3 groups, H atoms, and CO, respectively. Under the assumptions that reactions 1 through 3 and 5 through 7 are at equilibrium and that atomic oxygen is removed from the catalyst surface at the same rate that methane is formed, it has previously been shown (4,8) that θ_{CH_3}, θ_{CO}, and θ_H can be represented by

$$\theta_{CH_3} = \left(\frac{k_4}{k_8}\right)^{1/2} (K_2K_3K_5K_6K_7)^{1/2} \frac{P_{H_2}}{\theta_{CO}} \tag{5}$$

$$\theta_{CO} = K_1 P_{CO} \theta_v \tag{6}$$

$$\theta_H = K_3^{1/2} P_{H_2}^{1/2} \theta_v, \tag{7}$$

where k_i is the rate coefficient for reaction i, K_i is the equilibrium constant for reaction i, and θ_v is the fraction of the catalyst surface which is vacant. Furthermore, in situ infrared studies (6,14,15) indicate that

$$\theta_{CO} \simeq 1.0 \tag{8}$$

and

$$\theta_v = \frac{1}{K_1 P_{CO}} \tag{9}$$

Substitution of eqns. 5, 6, and 7 into eqns. 3 and 4, and elimination of θ_{CO} and θ_v from the resulting equations by substitution from eqns. 8 and 9, leads to the following rate expressions for methane and acetaldehyde:

$$N_{CH_4} = \frac{K_3}{K_1} (k_8k_4K_2K_5K_6K_7)^{1/2} \frac{P_{H_2}^{1.5}}{P_{CO}} \tag{10}$$

$$N_{CH_3CHO} = k_{12} \left(\frac{k_4}{k_8}\right)^{1/2} (K_2K_3K_5K_6K_7)^{1/2} P_{H_2} \tag{11}$$

It should be noted that eqn. 10 is identical to the expression derived in previous discussions of methane synthesis based upon the mechanism presented in Fig. 5 (4,8).

Comparison of eqns. 2 and 10 shows that the rate expression for methane synthesis obtained theoretically is in reasonably good agreement with that observed experimentally using the Ru/SiO_2 catalyst. A similar level of agreement is also noted for acetaldehyde synthesis, as may be judged by comparison of eqns. 1 and 11.

The mechanism outlined in Fig. 5 also provides a basis for understanding the origin of the inverse isotope effects observed for acetaldehyde and methane synthesis and the reason why the effect is larger for acetaldehyde. To proceed, we must first examine the influence of isotopic substitution on the factors entering into eqns. 3 and 4. A normal primary kinetics isotope effect is expected for reaction 8, since this reaction involves the addition of a hydrogen atom (16). Consequently, k_8^H should be larger than k_8^D. Since hydrogen is not involved directly in reaction 12, only a secondary kinetic isotope effect is expected, and k_{12}^H should be approximately equal to k_{12}^D. The only factor influencing the fractional surface coverage by hydrogen, which is sensitive to isotopic substitution, is K_3. An analysis of the ratio K_3^H/K_3^D based upon statistical mechanics (2) shows that $1.27 < K_3^H/K_3^D < 1.61$ for temperatures between 453 and 543K. Consequently, we can deduce from eqns. 7 and 9 that $\theta_H > \theta_D$.

Examination of eqn. 5 indicates that several factors will influence the relative magnitudes of θ_{CH_3} and θ_{CD_3}. The ratio of the rate coefficients for reactions 4 and 8 should contribute only a small effect since similar primary kinetic isotope effects are expected for reactions 4 and 8. Reaction 2 will not exhibit an isotope effect and the isotope effect on reaction 3 has

already been discussed. An inverse equilibrium isotope effect should occur for reactions 5 through 7, since these reactions involve the addition of a hydrogen atom to a C_1 intermediate in a reversible process (16). Taking all of the factors into account, and recognizing that the inverse isotope effect associated with the product $K_5K_6K_7$ should be larger than the normal isotope effect associated with K_3, it seems reasonable to expect that θ_{CD_3} will be larger than θ_{CH_3}.

The isotope effects predicted for k_8 and θ_{CH_3} in the preceding discussion can be confirmed by a comparison of the overall isotope effects associated with the formation of methane and acetaldehyde. As the first step in this process, eqns. 3 and 4 are combined to obtain eqn. 12.

$$N_{CH_4} = \frac{k_8 K_3^{1/2}}{k_{12} K_1} \frac{P_{H_2}^{1/2}}{P_{CO}} N_{CH_3CHO} \qquad (12)$$

The ratio N_{CH_4}/N_{CD_4} can then be expressed as

$$\frac{N_{CH_4}}{N_{CD_4}} = \frac{k_8^H}{k_8^D} \left(\frac{K_3^H}{K_3^D} \right)^{1/2} \frac{N_{CH_3CHO}}{N_{CD_3CDO}} \qquad (13)$$

Substitution of the experimentally determined values for N_{CH_4}/N_{CD_4} and N_{CH_3CHO}/N_{CD_3CDO}, and an average value for K_3^H/K_3^D of 1.43 (2) into eqn. 13, leads to an estimate of $k_8^H/k_8^D = 1.51$. The fact that the ratio of k_8^H to k_8^D is greater than unity is consistent with the nature of reaction 8, as discussed above. The relationship between θ_{CH_3} and θ_{CD_3} is obtained very simply. Inspection of eqn. 4 shows that $\theta_{CH_3}/\theta_{CD_3} = N_{CH_3CHO}/N_{CD_3CDO}$, so that $\theta_{CH_3}/\theta_{CD_3} = 0.5$. This result is consistent with the projection based on the analysis of eqn. 5 given earlier.

To summarize the analysis given here indicates that the isotope effects found for acetaldehyde and methane synthesis can be interpreted in terms of a product of equilibrium and kinetic isotope effects. The inverse isotope effect observed for acetaldehyde appears to be due totally to the inverse equilibrium isotope effect associated with the surface coverage by $CH_3(CD_3)$ groups. In the case of methane, the inverse isotope effect is due to a product of three factors: a normal kinetic isotope effect associated with reaction 8; a normal equilibrium isotope effect associated with the chemisorption of $H_2(D_2)$, reaction 3; and the inverse equilibrium isotope effect associated with the surface coverage by $CH_3(CD_3)$ groups. This last result is consistent with the projection given recently by Wilson (16) and subsequently confirmed by Kellner and Bell (2).

A possible mechanism for the formation of methanol, similar to that recently proposed by Kung (17), is shown in Fig. 6. In this instance it is proposed that CO hydrogenation proceeds without rupture of the C-O bond and that the first stage of this process involves the rearrangement of linearly-adsorbed CO to form a μ-bridge adsorbed structure. Species of this type are known to occur in transition metal complexes (18) and can also be formed by interaction of the oxygen and of a linearly-bonded CO ligand with a Lewis acid site (19). Furthermore, some evidence for the presence of bridge-adsorbed CO on Ru/Al_2O_3 has been obtained in recent infrared studies (15). Hydrogenation of the bridge-adsorbed intermediate is postulated to occur initially at the carbon end of the C-O bond. Continuation of this process produces a methoxy species which then undergoes reductive elimination to form methanol.

The results of the present studies of methanol synthesis over Ru/Al_2O_3 do not permit a detailed assessment of the extent to which the mechanism presented in Fig. 6 is correct. Nevertheless, it is significant to point out that the proposed scheme is consistent with two important observations. The first is the occurrence of a substantial increase in the rate of methanol synthesis (see Fig. 4) when D_2 is substituted for H_2 in the synthesis feed. This suggests that one or more of the hydrogenation steps (reactions 4-6 in Fig. 6) is at equilibrium (16). The second observation is that the yield of methanol declines as the flow rate of synthesis gas is reduced (see Fig. 2). As noted earlier, this implies that at lower flow rates the methanol concentration over the catalyst builds up and as a result methanol decomposition enters into competition with the synthesis of this product. Studies by Madix and coworkers have shown that methanol decomposition over Fe, Ni, and Pt (20,21) is initiated by the loss of the hydroxyl hydrogen and the concurrent formation of an adsorbed methoxy structure. Assuming that Ru behaves in a similar fashion to these other group VIII metals and that the concept of microreversability holds, we conclude that the last step in the formation of methanol proceeds as indicated in Fig. 6.

It is not possible at present to explain why acetaldehyde is produced as the primary oxygenated product over the Ru/SiO_2 catalyst while methanol is the primary oxygenated product formed over the Ru/Al_2O_3 catalyst. All that one can say is that interactions between the metal and the support alter the catalyst selectivity. Evidence for such effects have also been reported recently by Ichikawa and coworkers (22-25) for Rh, Pd, and Pt catalysts and by Ryndin et al. (26) for Pd catalysts. Unfortunately, the current understanding of the metal-support interactions is insufficient to warrant speculation concerning the manner in which these interactions affect catalyst activity and selectivity.

CONCLUSIONS

The present results demonstrate that under appropriate conditions Ru catalysts exhibits a significant activity for the formation of oxygenated products from CO and H_2. For Ru/SiO_2 the principal product observed was acetaldehyde. The kinetics of acetaldehyde synthesis and the observation of an inverse H_2/D_2 isotope effect can be explained in terms of a mechanism in which acetaldehyde is formed by insertion of CO across the metal-carbon bond of an adsorbed methyl group followed by reductive elimination of the resulting acetyl group. On the other hand, methane is formed by reductive elimination of the methyl group. Comparison of the rate expressions derived for acetaldehyde and methane synthesis, and the H_2/D_2 isotope effects for both products, makes it possible to estimate the individual kinetic and equilibrium isotope effects associated with the synthesis of each product.

When Ru is supported on γ-alumina, methanol is produced as the principal oxygenated species. This product readily decomposes back to CO and H_2 and hence the kinetics of methanol formation are sensitive to the methanol concentration in the products. The formation and decomposition of methanol can be explained in terms of a simple mechanism which involves the hydrogenation of μ-bridge-adsorbed CO to form a methoxy species. This group then undergoes reductive elimination to form methanol. The observation of an inverse H_2/D_2 isotope effect on the rate of methanol synthesis suggests that one or more of the initial hydrogenation steps is reversible and at equilibrium.

ACKNOWLEDGMENT

This work was supported by the Director, Office of Energy Research, Office of Basic Energy Sciences, Chemical Sciences Division of the U.S. Department of Energy, under Contract#W-7405-ENG-48.

REFERENCES

1. Storch, H. H., Golumbic, N., and Anderson, R. B., "The Fischer-Tropsch and Related Syntheses", Wiley, New York, 1951.

2. Kellner, C. S., and Bell, A. T., J. Catal., in press.

3. Kuznetsov, V. L., Bell, A. T., Yermakov, Yu. I., J. Catal. 65, 374 (1980).

4. Kellner, C. S., and Bell, A. T., submitted to J. Catal.

5. Dalla Betta, R. A., J. Phys. Chem. 79, 2519 (1975).

6. Ekerdt, J. G., and Bell, A. T., J. Catal. 58, 170 (1979).

7. Greenler, R. G., J. Chem. Phys. 37, 2094 (1962).

8. Bell, A. T., Cat. Rev.-Sci. Eng. 23, in press.

9. Calderazzo, F., Angew. Chem. Int. Ed. Engl. 16, 299 (1977).

10. Muetterties, E. L., and Stein, J., Chem. Rev. 80, 479 (1979).

11. Schrauzer, G. N., "Transition Metals in Homogeneous Catalysis", Dekker, New York, 1971.

12. Green, M. L. H., Mitchard, L. C., Swanwick, M. G., J. Chem. Soc. A, 794 (1971).

13. Headford, C. E. L., and Roper, W. R., J. Organometallic Chem. 198, C7 (1980).

14. Dalla Betta, R. A., and Shelef, M., J. Catal. 48, 111 (1977).

15. Kellner, C. S., and Bell, A. T., submitted to J. Catal.

16. Wilson, T. P., J. Catal. 60, 167 (1979).

17. Kung, H. H., Cat. Rev.-Sci. Eng. 22, 235 (1980).

18. Manassero, M., Sansoni, M., and Langoni, G., J. C. S. Chem. Comm. 1919 (1976).

19. Kristoff, J. S., and Shriver, D. F., Inorg. Chem. 13, 499 (1974).

20. Benziger, J. B., and Madix, R. J., J. Catal. 65. 36 (1980).

21. Madix, R. J., Department of Chemical Engineering, Stanford University, Stanford, CA, personal communication.

22. Ichikawa, M., J. C. S. Chem. Comm., 566 (1978).

23. Ichikawa, M., Bull. Chem. Soc. Japan 51, 2268, 2273 (1978).

24. Ichikawa, M., Shokubai 21, 253 (1979).

25. Ichikawa, M., and Shikakura, K., Preprints, The Seventh International Congress on Catalysis, Tokyo, July 1-2, 1980.

26. Ryndin, Yu. A., Hicks, R. F., Bell, A. T., and Yermakov, Yu. I., submitted to J. Catal.

Table I

The Effects of H_2/CO Ratio and Pressure on the Rates of Methanol and Methane Formation Over a 1.0% Ru/Al_2O_3 Catalyst at 498K

H_2/CO	P (atm)	N_{CH_3OH} (s^{-1})	N_{CH_4} (s^{-1})
3	10	1.5×10^{-3}	2.5×10^{-3}
3	5	9.7×10^{-4}	2.0×10^{-3}
3	1	2.4×10^{-4}	1.3×10^{-3}
2	10	9.7×10^{-4}	1.4×10^{-3}
2	5	7.0×10^{-4}	1.1×10^{-3}
2	1	1.4×10^{-4}	6.6×10^{-4}
1	10	6.0×10^{-4}	8.7×10^{-4}
1	5	3.4×10^{-4}	6.7×10^{-4}
1	1	7.3×10^{-5}	4.0×10^{-4}

FIGURE CAPTIONS

Fig. 1 Arrhenius plots for the synthesis of acetaldehyde and methane from $H_2(D_2)$ and CO over a silica-supported Ru catalyst

Fig. 2 Effect of feed flow rate on the rate of methanol synthesis over an alumina-supported Ru catalyst

Fig. 3 Effect of reaction time on the rates of methane and methanol synthesis over an alumina-supported Ru catalyst

Fig. 4 Arrhenius plots for the synthesis of methanol and methane from H_2CD_2 and CO over an alumina-supported Ru catalyst

Fig. 5 Proposed mechanism for the synthesis of hydrocarbons and acetaldehyde

Fig. 6 Proposed mechanism for the synthesis of methanol

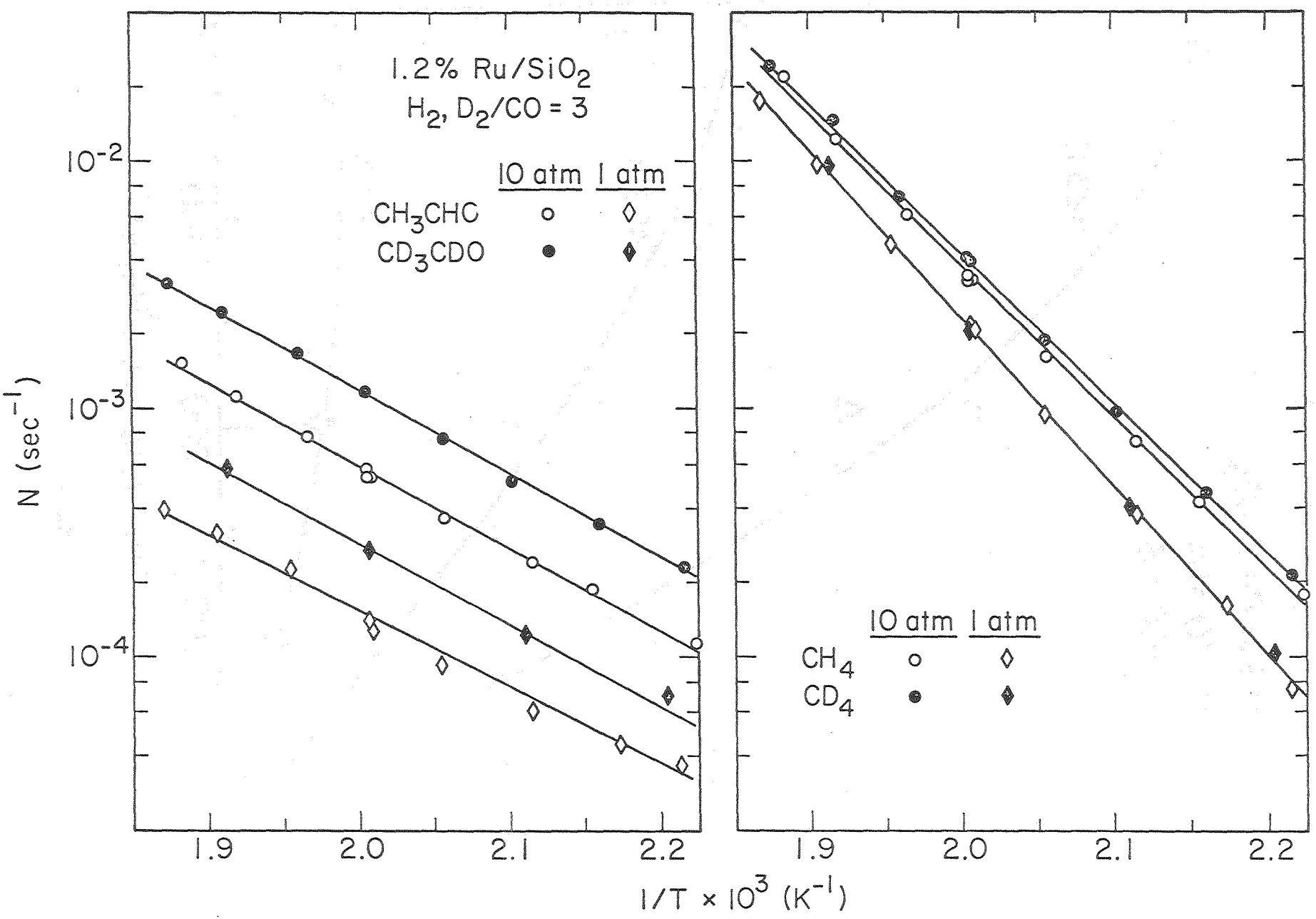
1.2% Ru/SiO2
H2, D2/CO = 3
10 atm
1 atm
CH3CHO
CD3CDO
CH4
CD4
N (sec-1)
1/T × 10^3 (K-1)
10-2
10-3
10-4
1.9
2.0
2.1
2.2

Fig. 1

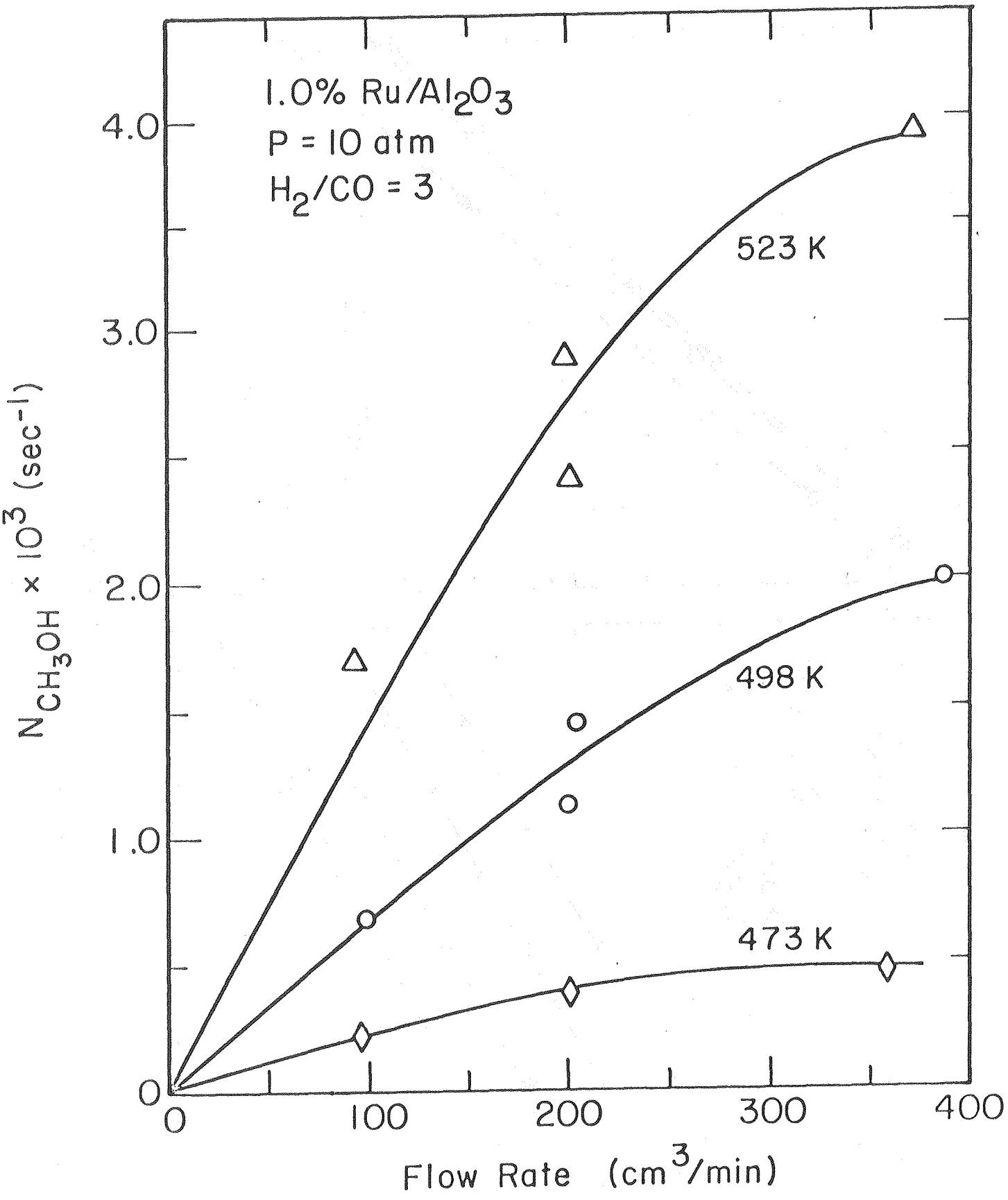
1.0% Ru/Al2O3
P = 10 atm
H2/CO = 3
523 K
498 K
473 K
4.0
3.0
2.0
1.0
0
0
100
200
300
400
N CH3OH x 10^3 (sec^-1)
Flow Rate (cm^3/min)

Fig. 2

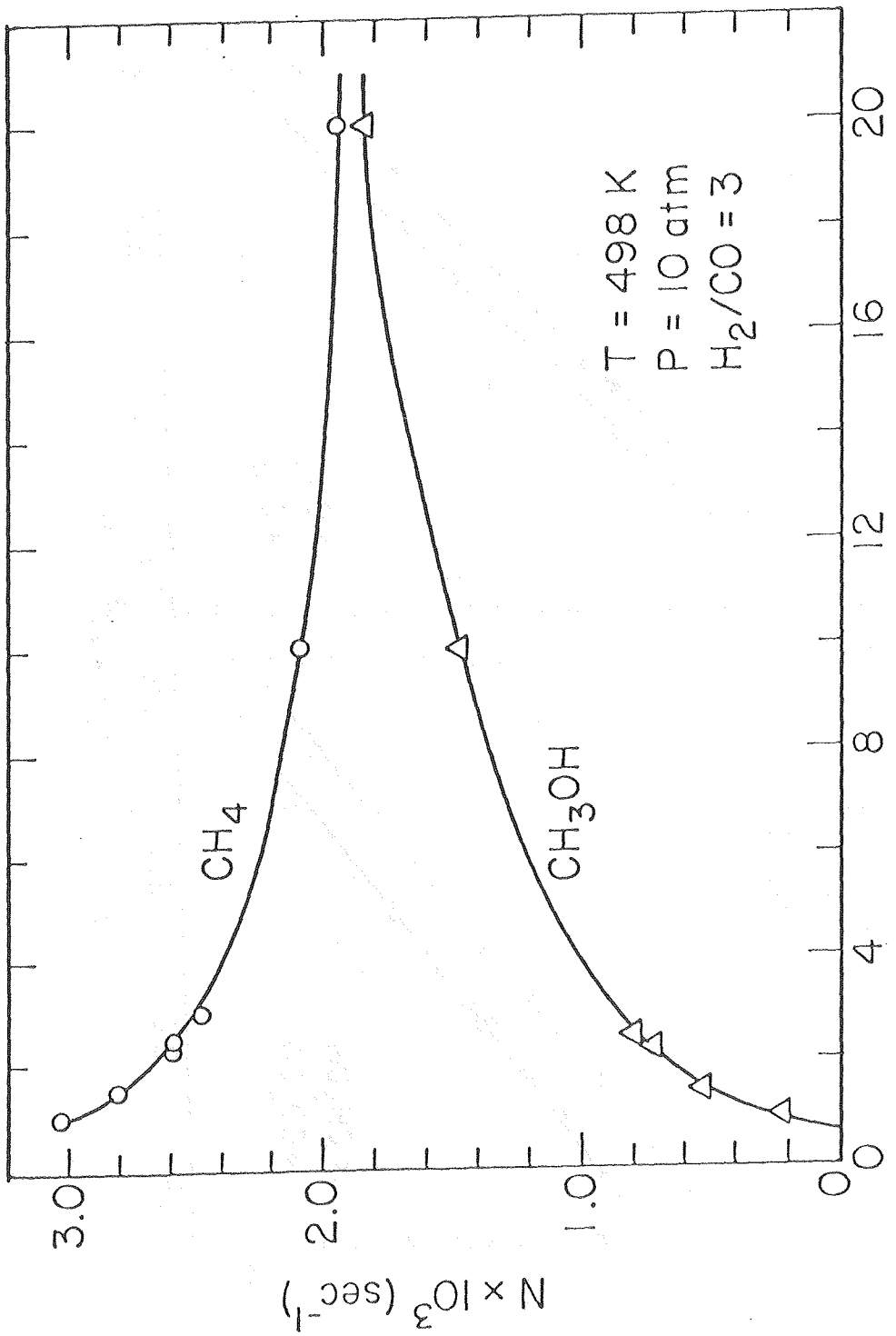
T = 498 K
P = 10 atm
$H_2/CO = 3$
CH_4
CH_3OH
$N \times 10^3$ (sec^{-1})
3.0
2.0
1.0
0
0
4
8
12
16
20
Time (min)

Fig. 3

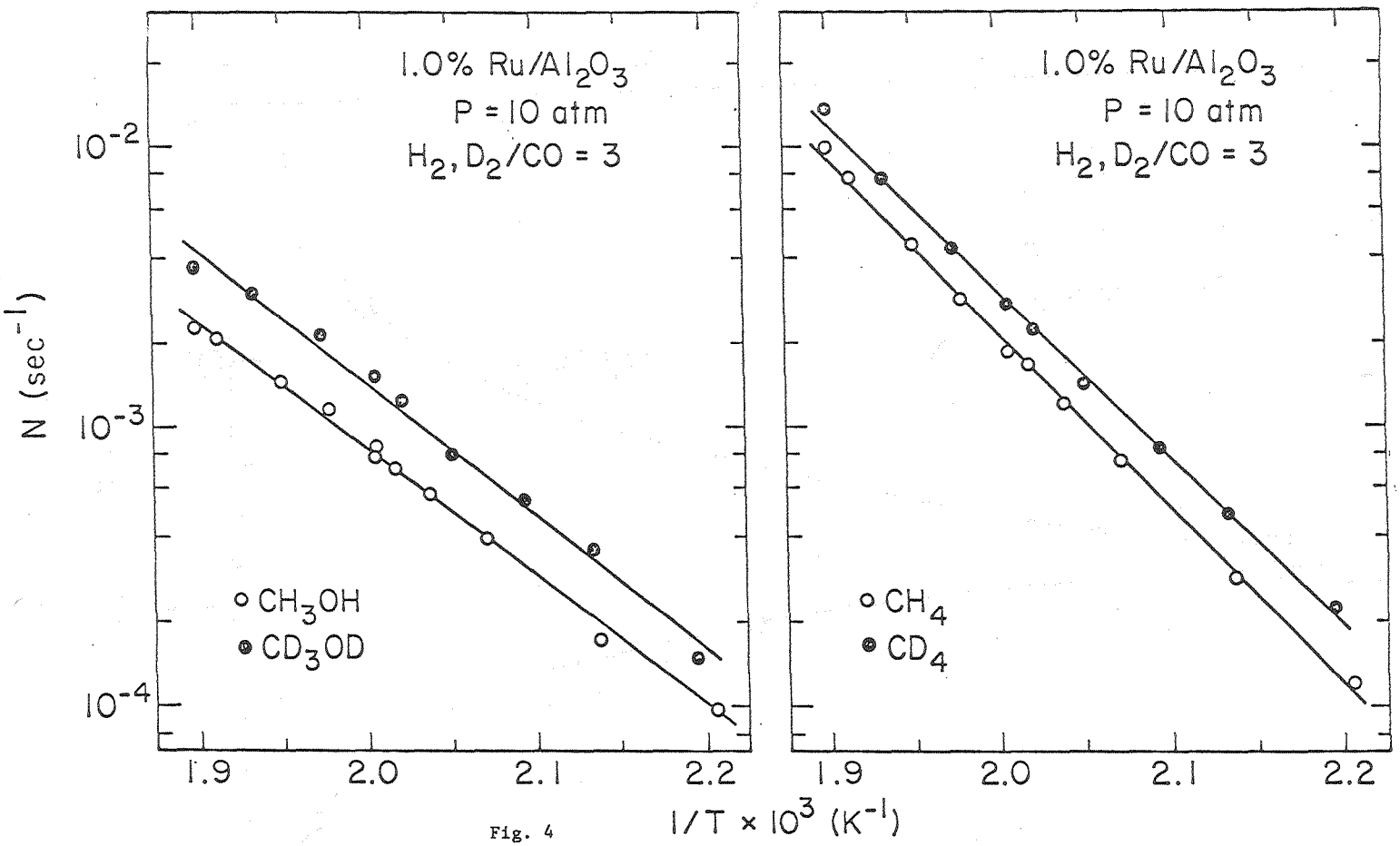
1.0% Ru/Al2O3
P = 10 atm
H2, D2/CO = 3
CH3OH
CD3OD
1.0% Ru/Al2O3
P = 10 atm
H2, D2/CO = 3
CH4
CD4
N (sec-1)
10-2
10-3
10-4
1.9
2.0
2.1
2.2
1/T x 10^3 (K-1)

Fig. 4

1. $CO + S \rightleftharpoons CO_s$
2. $CO_s + S \rightleftharpoons C_s + O_s$
3. $H_2 + 2S \rightleftharpoons 2H_s$
4. $O_s + H_2 \rightarrow H_2O + S$
5. $C_s + H_s \rightleftharpoons CH_s + S$
6. $CH_s + H_s \rightleftharpoons CH_{2_s} + S$
7. $CH_{2_s} + H_s \rightleftharpoons CH_{3_s} + S$
8. $CH_{3_s} + H_s \rightarrow CH_4 + 2S$
9. $CH_{3_s} + CH_{2_s} \rightarrow C_2H_{5_s} + S$
10. $C_2H_{5_s} + S \rightarrow C_2H_4 + H_s + S$
11. $C_2H_{5_s} + H_s \rightarrow C_2H_6 + 2S$
12. $CH_{3_s} + CO_s \rightarrow CH_3CO_s$
13. $CH_3CO_s + H_s \rightarrow CH_3CHO + 2S$
14. $C_2H_{5_s} + CH_{2_s} \rightarrow C_3H_{7_s} + S$

etc.

Fig. 5

1. $CO + S \rightleftharpoons S-C\equiv O$
2. $S-C\equiv O + S' \rightleftharpoons S-C\equiv O \cdots S'$
3. $H_2 + 2S \rightleftharpoons 2H_s$
4. $S-C\equiv O \cdots S' + H_s \rightleftharpoons S-\overset{H}{C}=O \cdots S'$
5. $S-\overset{H}{C}=O \cdots S' + H_s \rightleftharpoons S-CH_2-O-S'$
6. $S-CH_2-O-S' + H_s \rightleftharpoons S + CH_3-O-S'$
7. $CH_3O-S' + H_s \rightleftharpoons CH_3OH + S' + S$

Fig. 6